



A novel hybridised composite sandwich core with Glass, Kevlar and Zylon fibres – Investigation under low-velocity impact

Sartip Zangana^{a,*}, Jayantha Epaarachchi^a, Wahid Ferdous^b, Jinsong Leng^c

^a University of Southern Queensland, Centre for Future Materials (CFM), School of Mechanical and Electrical Engineering, Toowoomba, QLD 4350, Australia

^b University of Southern Queensland, Centre for Future Materials (CFM), Toowoomba, QLD 4350, Australia

^c Centre of Composite Materials and Structures, Harbin Institute of Technology, Harbin, China

ARTICLE INFO

Keywords:

Sandwich core
Glass
Kevlar and Zylon fibres
Low-velocity impact
Damage modes
Energy absorption

ABSTRACT

A novel fibre composite sandwich core has been introduced in this study. Trapezoidal corrugated core glass-fibre sandwich structures were hybridised using Kevlar and Zylon fibres to improve the dynamic impact performance. The composite cores were fabricated with four layers of glass fibre and one of the layers was replaced either by Kevlar or Zylon fibre to create hybrid composite core (Glass-to-Kevlar or Glass-to-Zylon ratio 75:25). The impact behaviour, damage mode, specific absorbed energy, and residual strength after the impact of the composite sandwiches were investigated using a low-velocity impact test with 30 J, 40 J and 50 J kinetic energy level. The experimental results revealed that the hybridised sandwiches with high-performance fibre are performing extremely well when subjected to impact energy above the threshold limit. The observations during the experimental work and numerical simulation have confirmed that Glass-Kevlar and Glass-Zylon hybridisation can eliminate severe core rupture by minimising stress concentration and provide high specific energy without increasing structural weight. Moreover, the loss of strength and stiffness of trapezoidal corrugated core sandwich structures after an impact event can be minimised up to 56% and 69%, respectively using Glass-Zylon hybridisation technique. Furthermore, an empirical relationship for predicting the residual strength of the composite core sandwich is proposed.

1. Introduction

The application of sandwich structures increased extensively in aerospace, marine, automotive, and transportation industries as well as civil constructions [1]. Sandwich structures are often subjected to low-velocity impact during their service life. This impact may arise from the falling tools during maintenance work, bird strike, runway debris, tire rubber impact, fan engine blade-off, hail storm, and water ditching in particular if they are used in aircraft or marine applications. Several researchers aimed to improve impact performance (high stiffness and lightweight, high impact resistance, and energy absorption) and minimise damage size, particularly core damage of such sandwich panels under low-velocity impact [2,3]. Their approach mainly focused on core configurations such as traditional metal-based honeycomb core [4], sandwich metal foam cores [5], triangular core filled with ceramic [6], lattice truss pattern and Y-frame core [7–10], multilayer corrugated core [11,12], sinusoidal core [13,14], aluminum Bi-tubular corrugated sandwich [15], and corrugated core sandwich [16,17]. Among them, corrugated core sandwich structures gained particular attention

due to their anisotropic mechanical properties [18], high strength/stiffness-to-weight ratio [17,19–21] and relatively high impact energy absorption capacity [11,22]. This type of folded core also minimise the problems related to the humidity retention (common in foam core) due to their excellent ventilation characteristics while their efficient in-line production technology leads to reduce the cost. Another approach is to combine polymeric or metal and fibre composite materials in the fabrication of sandwiches to improve impact resistance and minimise damage size. For example, studies have been conducted on the composite face sheet with 3D-printed polymeric core [23, 24], aluminium corrugated core [25], hybrid corrugated core sandwich [26], plywood core with aluminium skins [27], kagome titanium truss core with carbon face sheet [28], aluminium core with carbon face sheet [29], aluminium honeycomb core with woven glass fabric epoxy laminate face sheet [30] and aluminium corrugated core with carbon face sheets [31]. However, the aforementioned studies hybridised the face sheets but not the core materials, and this approach marginally improved the impact capacity. Therefore, an improved engineering approach is deemed necessary to improve the impact capacity.

* Corresponding author.

E-mail address: Sartip.Zangana@usq.edu.au (S. Zangana).

The increase of impact resistance with minimal sandwich weight is an essential design criterion for sandwich structures [32]. To achieve that the researches are now focusing on fibre composite cores along with fibre composite face sheets for the sandwich systems. The present study focused on improving fibre composite cores instead of face sheets. The study on two-layers carbon-fibre composite pyramidal core observed an improved energy absorption capability and less damage in the sandwich [33]. Schneider et al. [34] fabricated the wrapped fibre composite corrugated core and tested under out-of-plane dynamic loading conditions. They observed the suppression of the failure modes due to the warped fibre, while the high core density showed limited rate sensitivity. Shi et al. [35] improved sandwich properties of thin-walled honeycomb by adding an orthogrid structure in the core to minimise core crushing. While these concepts can minimise the overall weight, but the structural performance under impact load is remained a critical issue. To overcome this limitation, the researches should focus on the entire sandwich system with high-performance composite fibres.

One engineering approach to improve the impact resistance of the composite core without increasing weight/thickness is to combine the traditional fibres with high strength fibres. Zylon, a high-performance fibre has recently been introduced in the market. This fibre offers a high tensile strength, which is 1.6 times more than Kevlar with similar density, and twice strength but only 20% density of steel fibre [36]. The extremely high ultimate tensile strength (UTS), high elastic modulus and good electrical insulation may improve impact resistance without increasing structural weight [37]. However, the extensive survey of literature only found some mechanical characteristics study [37,38], but no investigation has been reported on the impact performance of Zylon fibre. This is probably due to the recent development of this fibre compare to the traditional fibres such as carbon and glass. Therefore, it is worthwhile to investigate how Zylon fibre can perform under low-velocity impact.

This study investigated the combination of different fibers (Glass, Kevlar, and Zylon) in the fabrication of trapezoidal corrugated core of the sandwich systems with the aim to achieve the superior performance in specific stiffness/strength, energy absorption, and core damage without increasing structural weight/thickness under low-velocity impact. The performance of glass-Zylon was compared with the Glass-Kevlar and the traditional Glass-Glass combinations. Three different ply combinations and energy levels were studied to achieve the goals. The residual strength after the impact of the corrugated core sandwiches was also investigated in order to understand their damage levels. The outcome of this study will help in designing high-performance and lightweight trapezoidal composite corrugated core sandwich structures.

2. Manufacturing of corrugated sandwich

Three types of trapezoidal composite corrugated core sandwich named as GG (Glass-Glass), GK (Glass-Kevlar), and GZ (Glass-Zylon) were fabricated in this study. The trapezoidal composite corrugated core sandwich panels were manufactured in four steps. First, four-ply of woven E-glass fiber were stacked to fabricate the upper and lower skins of the sandwiches. Then three different types of corrugated core were manufactured in a prefabricated wood mould. The wooden mould was made with an isosceles trapezoid cross-section to fabricate the composite corrugated core with the corrugated pitch of (L) of 120 mm, short span length of (L₁) 30 mm, long span length of (L₃) 90 mm core height (h) of 30 mm and an inclination angle (w_1) of 45° (Fig. 1a). To ensure de-molding, the wooden profile was covered with a sticky Nylon film. The fiber composite laminates were fabricated by hand lay-up technique. The warp yarns laid in the Z direction (i.e., remained straight), and the weft yarns of the fabric were bent over the corrugated core profile edges in the X-direction. A constant load used to press corrugated mould for no less than 48 h at room temperature (20 °C).

Fig. 1(b) shows the schematic profile of the stacking sequence of the fibre layers in the core configuration. The first core configuration (GG)

were made by using just woven E-glass fibre. In the second corrugated core configuration, three layers of woven E-glass fibre and one layer of Kevlar fibre were used to fabricate hybrid Glass-Kevlar core (GK), i.e., Glass-to-Kevlar ratio 75:25. The same procedure was used in the fabrication of the third corrugated core, three plies of woven E-glass fibre stacked with one layer of Zylon fiber to fabricate hybrid Glass-Zylon corrugated core (GZ), i.e., Glass-to-Zylon ratio 75:25. Increasing the high-performance fibre volume fraction above 25% (such as Z-G-Z-G or Z-Z-Z-Z) would lead to increase the impact capacity however, the fabrication cost of the core will also increase. Therefore, the required number of Zylon layers is dependent on the performance and cost criteria of the sandwich core. To utilise the benefit of Zylon or Kevlar for impact resistance, the high-performance fibres need to be placed as close as to the impact surface. As such the exterior layer of the core should be made up of high-performance fibre. However, the fibre layers at the contact surface between face sheets (both upper and lower) and the core have to be similar to ensure proper bonding. Because of this reason, the second layer (i.e., G-Z-G-G) was fabricated using the high-performance fibre. The mechanical properties of the fibre plies and resin system are summarised in Table 1. In the third step, the fabricated parts glued together by using Techniglu (R5-H5). The proper selection of the glue is an essential criterion to avoid the micro-cracking that can occur due to the stress transfer between fibre and the bond surface. The glue [39] that used in this study has high resistance to micro-cracking damage and compatible with matrix resin used to manufacture the composite. Finally, the sandwich panels were cut to the required dimensions for testing. Table 2 shows the types of composite corrugated core sandwich panels and their weights.

3. Experimental program

3.1. Impact tests

Drop-weight impact tests, as a rule, involve an impactor weight and impactor head that falls along with guideposts and collides with the target. In this study, the drop-weight test was conducted on composite corrugated core sandwich structures by using the hemispherical head (diameter = 12 mm) connected to three different impactor masses (m) with constant impact velocity ($v = \sqrt{2gh}$) to obtain three different kinetic energies ($K. E = \frac{1}{2}mv^2$), where g is the gravity, h and m are the height and impactor mass, respectively. This study only considered the impact on short span of the core as there were no major changes observed by Liu et al. [45] in impact behaviour due to the variation of impact location (i.e., short span and long span). Table 3 shows the impactor mass, initial impact velocity and kinetic energy applied on the specimen.

The low-velocity impact tests were conducted according to the standard guidelines specified in ASTM D7136 [46]. The kinetic energy was decided using $E = h \cdot C_E$, where, h is the specimen thickness, E is the potential energy of impactor head prior to dropping (J) and C_E is the specific ratio of impact energy to specimen thickness (6.7 J/mm) [46]. The specimen thickness (3.3 mm) at the location of impact is the sum of upper skin thickness (1.8 mm) and an upper flat component of the core (1.5 mm). The kinetic energy of the first test set-up (i) is 30 J, which was set marginally above the threshold of damaged energy (22 J) of the composite laminate. This is to ensure the visibility of damage in the composite laminates under low-velocity impact. To simulate the low-velocity impact from incidents like dropped tools during service and maintenance, and intermediate-velocity impact of debris [47], the kinetic energy was increased to 40 J and 50 J for the set-up ii and iii (Table 3), respectively. One specimen in each category was tested as the previous investigation by the authors were found consistent results. According to Jang et al. [48] theory, the corrugated core sandwich specimens can be laid horizontally on a base plate and clamped only two sides using a jaw clamp. A corrugated core sandwich was mounted,

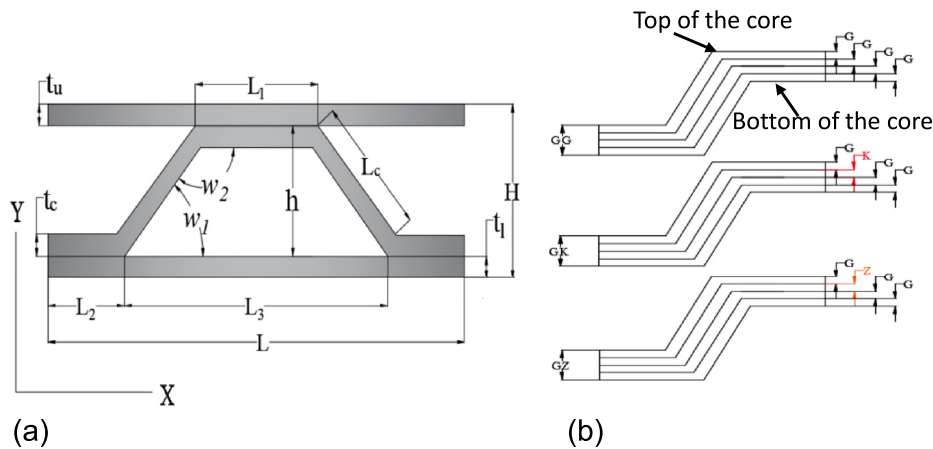


Fig. 1. Corrugated core sandwich (a) schematic diagram, and (b) ply order of the corrugated core for GG, GK, and GZ sandwich.

Table 1
Mechanical properties of the woven E-glass, Kevlar, and Zylon fibre.

Properties	Unit	Glass	Kevlar	Zylon	Epoxy	Reference
Density	g/cm ³	2.54	1.45	1.56	1.54	[40–43]
Tensile modulus	GPa	72	109	270	3.5	[40–43]
Shear modulus	GPa	30	2.9	2	1.25	[43,44]
Poisson's ratio		0.22	0.35	0.20	0.33	[43]
Tensile strength	GPa	3.4	3.6	5.8	0.06	[40–43]
Elongation at break	%	4.8	2.4	2.5	6.1	[40–42]

Table 2
Core thickness and density of composite corrugated core sandwich panels.

Sandwich type	Average core thickness, t_c (mm)	Average sandwich density, kg/m ³
GG- sandwich	1.50	259
GK- sandwich	1.45	243
GZ- sandwich	1.55	250

Table 3
Drop-weight test set-up configurations.

Set-up	Impactor mass (kg)	Impactor velocity (m/s)	Kinetic energy (J)
i	3	4.47	30
ii	4	4.47	40
iii	5	4.47	50

and two wood parts were attached between upper and lower face sheets of the structure to adjust the movement of the upper skin sheet. An LMS SCADAS system was used for data acquisition. A piezoelectric load sensor model (PCB 200C20) was set in between the impactor load and impactor head while PCB (5014B) accelerometer was employed to obtain the impact acceleration. A high-speed camera (Sony RX100) was used to capture the impact event and the deformation of all structural members. The data were recorded and stored for post-processing. Fig. 2(a) illustrates the drop weight impact tower and necessary equipment.

3.2. Bending after impact (BAI) test

Four-point bending tests on non-impacted (NI) and impacted composite corrugated core sandwiches were performed according to ASTM D5467 standard [49]. The third point loading span configuration (i.e., 4-point third span) with a total span of 150 mm, as shown in Fig. 2(b) has been used in accordance with ASTM-C393 standard [50]. The tests

were conducted using MTS testing machine with a capacity of 10 kN at a displacement rate of 0.5 mm/min, as shown in Fig. 2(b). Quantum XMX1615B - strain gauges bridge amplifier was used for strain measurement. Strain gauges (type FLA-5-11) were attached on the top surface of the upper face sheet beside the damaged trace in parallel to the corrugated core direction (i.e., Machine direction) as shown in figure Fig. 2(b).

4. Results and discussion

4.1. Effect of ply combination on impact response

Fig. 3(a) shows the impact response of the GG, GK, and GZ fiber-reinforced epoxy composite corrugated core sandwich structure subjected to 30 J of kinetic energy. It can be seen that all sandwich types exhibited similar impact response under low level of kinetic energy. The peak value and the corresponding impact time showed an identical magnitude. The force curve trace showed a sharp linear increase with increase the impact time until the peak load. Before reaching the peak value, the force-time trace showed a tiny drop between 1000 and 1500 N due to thin core thickness, which is prone to buckling. With further increase of impact time, the kinetic energy mitigated and impact force response gradually went down due to deformation of the sandwich and elastic buckling of the core (Fig. 3b–d). At the time between 0.004 and 0.006 s, the impact force exhibited an oscillation due to the degradation of the materials' stiffness at the upper face sheet leading to the local damage under the impactor nose. It can be seen that the high-performance fabric has no potential effect on sandwich impact behaviour at a low level of impact energy. Therefore, it is worthwhile to see the response at higher kinetic energy.

Fig. 4(a) illustrates force versus time response of the composite corrugated core sandwich impacted by 40 J kinetic energy. It can be seen that the sandwiches exhibited different responses at the kinetic energy of 40 J. For GG sandwich, the first stage ended at a time of 0.008 s that reflects the sandwich resistance until the core fracture, and then the force increase again to about 500 N. The phenomenon of the later stage is due to flexural bending resistance of the upper face sheet. For GK sandwich, the response after the peak force showed a plateau longer time compared to the GG sandwich. This is due to the large elastic core bulking followed by local core damage (Fig. 4c). However, the GZ sandwich exhibited a better response due to the core enhancement by high-performance fibre ply. Moreover, the GZ sandwich exhibited an increase in the impact resistance with no core damage (Fig. 4d).

Fig. 5(a) shows the impact response of the fabricated corrugated sandwiches under 50 J of impact energy. The GG and GK sandwich

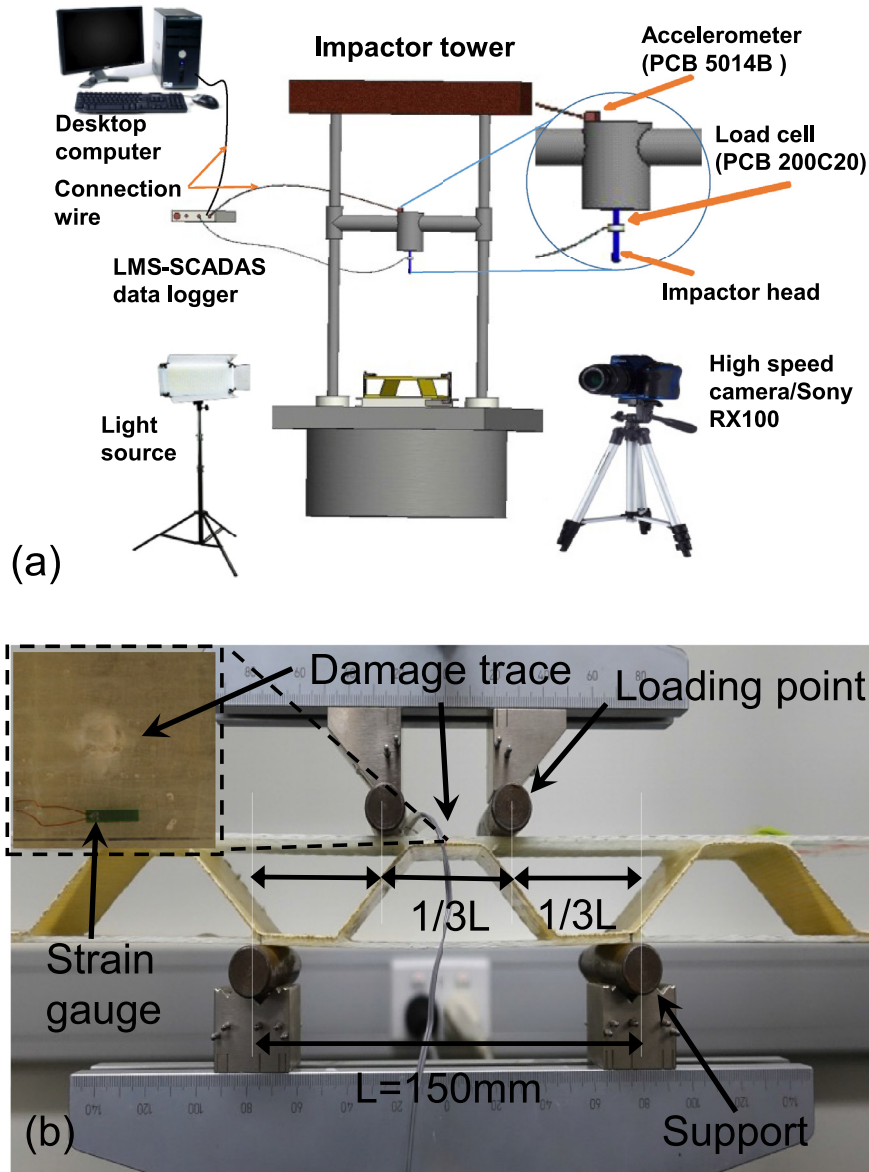


Fig. 2. Experimental set-up: (a) impact tower and the data logger; (b) four-point bending test set up after low-velocity impact on the sample.

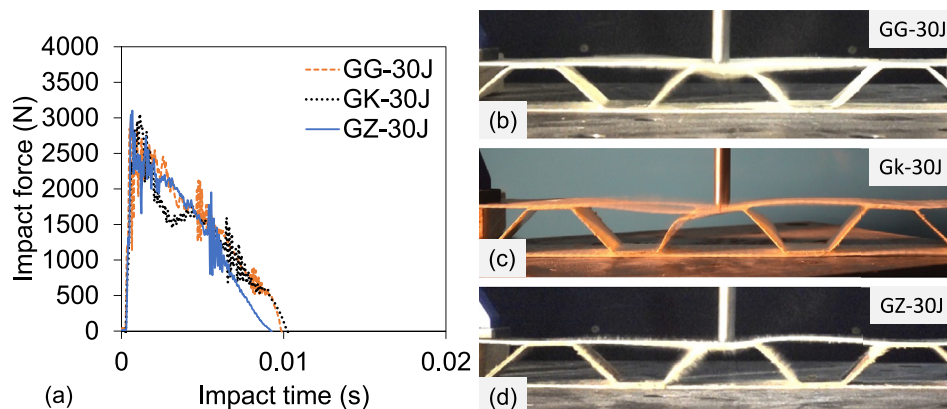


Fig. 3. GG, GK, and GZ corrugated core sandwich subjected to 30 J (a) impact force-time response, and (b-d) captured image at the end of the impact.

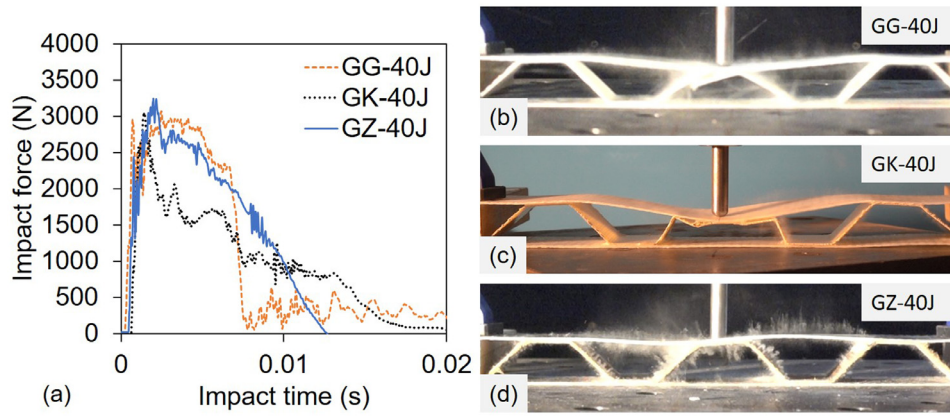


Fig. 4. GG, GK and GZ corrugated core sandwiches subjected to 40 J (a) impact force-time response, and (b–d) captured image at the end of the impact.

exhibited comparable force-time response at 50 J. Fig. 5(b) to (c), the GG and GK sandwich showed corrugation angle fracture and core buckling damage, respectively. The peak force of sandwich GZ also linearly increased, then the force dropped due to elastic core buckling and upper face deformation (Fig. 5d). Moreover, the force response showed the reparted fluctuation of the force due to the local external damage of the upper face sheet plies. Furthermore, the dust plumes on the sandwich members indicated the contribution of the adjacent core in resisting impact force. In general, one layer of Kevlar ply can improve sandwich resistance up to 3% (from 2968 N to 3055 N) at 30 J, 5% (from 2909 kN to 3056 kN) at 40 J and 7% (from 3015 kN to 3220 kN) at 50 J. On the other hand, one layer of Zylon ply can improve sandwich resistance up to 5% (from 2968 kN to 3101 kN) at 30 J, 12% (from 2909 kN to 3242 kN) at 40 J and 25% (from 3015 kN to 3759 kN) at 50 J. Therefore, it can be concluded that the high-performance Zylon fibre has only minimal influence up to the threshold impact energy (22), but it can improve the impact resistance of the corrugated core sandwich at high impact energy incidents. The impact resistance of Zylon fibre reinforced core has shown a superior impact resistance compared to glass and Kevlar at high energy impact situations.

4.2. Effect of ply combination on failure modes

The failure mode is one of the important criteria for designing any engineering structures. Therefore, it is important to inspect the composite corrugated core sandwiches after the impact event. A non-destructive examination was performed with the naked eye to understand the failure mode. Various types of damages and failure modes were revealed, such as white trace and upper face indent due to stress

Table 4

Damage and fracture modes of the composite corrugated core sandwich under different impact kinetic energy.

Specimen ID	White trace	Debonding failure	Core rupture upper angle	Core buckling fracture	Upper skin indent
GG-30J	x	o	o	o	o
GK-30J	x	o	o	o	o
GZ-30J	x	o	o	o	o
GG-40J	x	x	**	o	o
GK-40J	x	x	o	x	o
GZ-40J	x	x	o	o	x
GG-50J	x	x	**	o	o
GK-50J	x	x	o	x	o
GZ-50J	x	x	o	o	x

Note: (o) refers to no damage, (x) refers to damage, and (***) refers to a severe fracture.

concentration at the impacted area. The de-bonding of the upper face sheet and the upper flat core member also emerged as a major failure mode. Moreover, the core shear failure or core sturts damage appeared due to global buckling. In some cases, the combined damage modes were observed. Table 4 summarises the damage and fracture modes of the different corrugated core sandwich under the low-velocity impact. This table indicated that all the sandwich types exhibited a white circular damage trace on the upper face sheet due to matrix damage at 30 J kinetic energy. However, other members of the corrugated core sandwich have shown no noticeable damage trace.

The sandwich types GG, GK, and GZ showed de-bonding of the

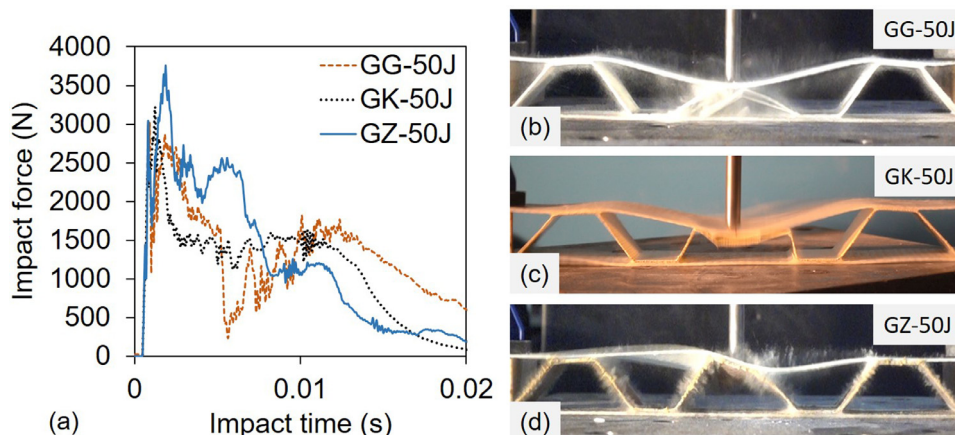


Fig. 5. GG, GK, and GZ corrugated core sandwich components subjected to 50 J (a) impact force-time response, and (b–d) captured image at the end of the impact.

upper face with a flat core member at an increasing impact energy of 40 J and 50 J. Moreover, the GG sandwich depicted severe core shear failure (severe internal core fracture) at the upper angle for the impact energy of 40 J and 50 J. This is due to exceed the limit of threshold shear stress of the core, and inertial stabilisation of the core struts. On the other hand, GK sandwich structure exhibited global core bulking associated with the core strut damage at the middle section of the web for the same level of impact energy. Although an external damage trace was clearly observed on the upper face sheet of the hybrid GZ corrugated core sandwich, discernible damages were not found in internal core members. This indicates that only one layer of Zylon ply enhanced impact resistance by preventing core crushing. Moreover, the GZ sandwich converted most of the impact energy to large deformation to maintain structural integrity. Similarly, the GZ sandwich showed significant superiority on the hybrid carbon aluminium corrugated core sandwich [29] by preventing penetration effect under low-velocity impact at 50 J kinetic energy. In summary, the rupture of the upper corrugation angle was the acute failure mode of the GG sandwich, which was eliminated by Kevlar and Zylon ply. Moreover, GZ prevented most of the damage by absorbing impact energy compare to GG and GK sandwich. The failure of GZ was external as evident by the damage on the upper face sheet while the GG sandwiches exhibited severe internal damage that is difficult to detect by visual inspection.

4.3. Effect of impact energy on damage area

Due to employing of the high-performance fibre in fabricating the sandwich panel subjected to low-velocity impact, it is important to correlate external damage area (i.e., indentation damage of the upper skin) and the kinetic energy. Fig. 6 shows that the increase of the kinetic energy increases the impact trace for all sandwiches; however, the slope of the GZ sandwich cores is steeper than the other two configurations. This indicates that the GZ sandwich cores distributed the impact force in a wider area than GK and GG at the same level of kinetic energy. This can be further examined in Fig. 7, which shows that the GG, GK, and GZ roughly exhibited similar magnitude of the impact area ranged from 12 to 17 mm² at the low kinetic energy of 30 J. At kinetic energy of 40 J and 50 J, the impacted area of the GG sandwich showed minimal magnitude when comparing with GK and GZ. This is due to early severe damage of the upper corrugation angle. The core buckling and the delay in core struts damage slowly increased the indentation area on the GK sandwich at 40 J and 50 J (Fig. 7). However, the high shear resistance of the Zylon fibre ply led to prevent internal core damage; thus, it transferred all impact energy (40 J and 50 J) in the wider area that increased local contact damage on the upper skin sheet

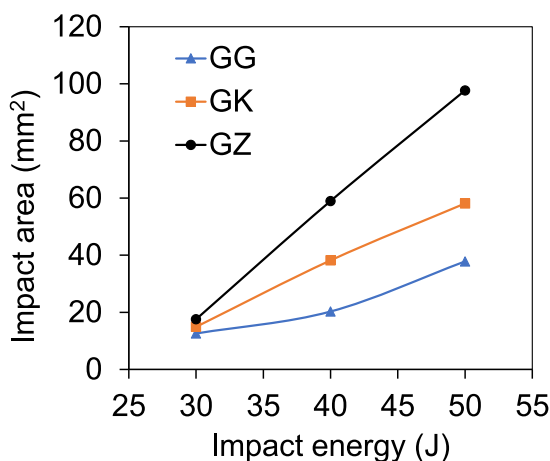


Fig. 6. Impacted area of the upper face sheet of GG, GK and GZ composite corrugated core sandwich with respect to the kinetic energy.

(Fig. 7). Using the high-stiffness synthetic fibre leads to a decrease in the common internal core crushing, enhancing the sandwich impact behaviour, and distributing the resulting stresses on the upper face sheet to external damage. The advantage here is that the upper face sheet can be repaired easily after any impact situation.

4.4. Effect of ply combination on specific energy absorption

Since the sandwich core structures exposed to impact events during their service life, the understanding of the specific energy absorption (SEA) capacity is an important aspect for their design. SEA is often employed to compare the performance and weight benefits in a light-weight design. Normalising the total absorbed energy by the sandwich weight leads to obtaining the specific absorbed energy ($SEA = AE/w$) in J/g. Where AE represents absorbed energy (i.e., total area under the force-displacement curve) and w is the sandwich weight. Fig. 8 shows the comparison of the specific absorbed energy of the corrugated sandwich under different kinetic energy. The GG sandwich exhibited roughly similar specific energy absorption with the increase of impact energy from 30 J to 50 J. However, the corrugated sandwich containing high-performance fibre plies showed a significant increase of SEA with the increase of impact energy. The increasing magnitude of SEA for the GZ sandwich indicates that it is more effective in designing sandwich structures at high impact energy. Furthermore, Table 5 compares the SEA from the current study with other types of core sandwiches under low-velocity impact from the literature. In Table 5, it is found that the GK and GZ can offer better specific energy than the other traditional core materials such as expanded polypropylene, aluminium, rubber and plastic. Employing high-performance synthetic fibres in the corrugated core sandwich can provide high specific energy while maintaining the lower weight.

This improvement of SEA in hybrid core is due to the fact that the Zylon ply minimised stress concentration at the location of upper core angle and transferred impact energy in a wider area. The high shear and tensile strength of Zylon fibre prevented internal core damage caused by combined shear and bending stresses produced from localized rotation of the upper angle. This phenomena has been examined using finite element simulation. Three-dimensional (3-D) finite element model was created by explicit dynamics ANSYS- workbench to investigate the stress distribution pattern of the GG and hybrid GZ composite sandwich core under low-velocity impact. The models built with the same geometry of the tested corrugated cores using ACP-pire code, then they exported to the workbench-explicit dynamic. The mechanical properties of the materials are summarised in Table 1. The properties were assumed same in both longitudinal and transverse directions due to 0/90 woven fibre orientations. The maximum failure criteria was employed to identify the failure or understand the high-stress zone. The maximum failure criteria value is ranged between 0 and 1 that implies no-damage and fully damage, respectively. The mesh was created with approximately 18000 SHELL181 elements with an aspect ratio of the elements were maintained close to one. A rigid and frictionless contact of impactor head was created using SOLID185 element as there was no visible deformation observed during the experimental program. The translation and rotation at the support of core were restricted to simulate the experimental setup and large geometric deformations were enabled. The impactor velocity and mass were 4.47 m/s and 5 kg, respectively to ensure 50 J of kinetic energy. The impactor was allowed to move in the Z direction and restricted in X and Y directions.

Fig. 9(a) and 9(b) shows the stress distribution based on maximum failure criteria of the GG and GZ composite sandwich core. Due to the stress concentration, it can be seen that the upper angle of the core (w_2) exhibited severe damage along the core angle (see Table 4). However, hybridisation of the glass fibre and high-performance Zylon fibre has distributed the stress on a larger area of the core, as shown in Fig. 9(b) due to high shear and tensile strength of the Zylon fibre. The finite element simulation showed a similar pattern of damage observed in the

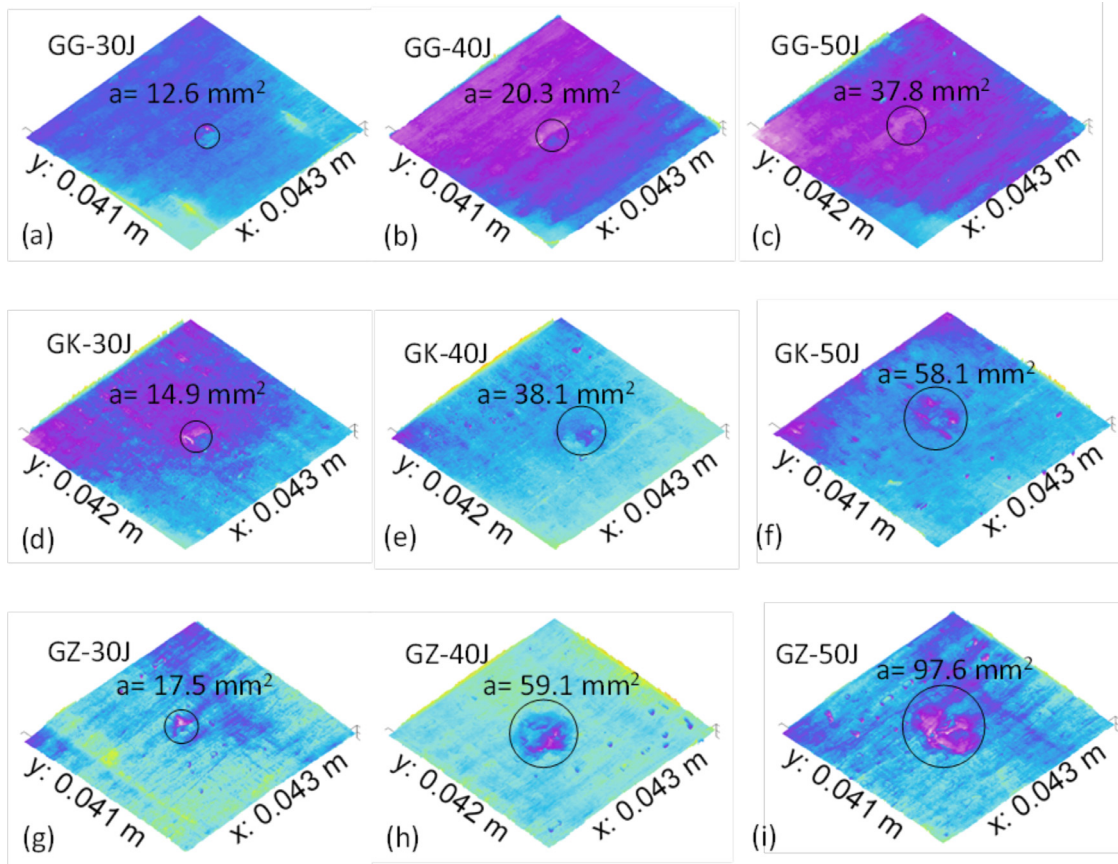


Fig. 7. Impact trace of GG, GK, and GZ sandwich under different impact energy analysed by Gwyddion code.

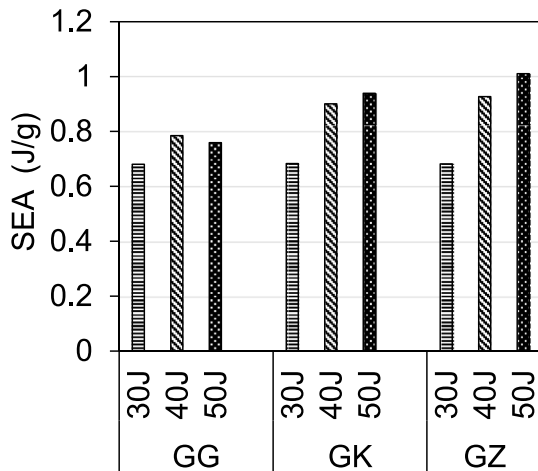


Fig. 8. Comparison of specific energy for different corrugated sandwiches.

experimental program.

4.5. Effect of ply combination on residual load-carrying capacity

Four-point bending test was conducted on non-impacted (NI) and impacted composite corrugated core sandwiches to measure the residual static load carrying capacity of the specimen. The specified test setup transmitted loads into the core from the upper face sheet. The bending tests were carried out according to ASTM-D5467 [49] standard. The tests were stopped after hearing the first crushing sound of the sandwich. Fig. 10 shows the force-displacement response of the GG, GK, and GZ sandwiches after impact. All the impacted sandwiches at

Table 5

Comparison of specific energy absorption among different materials.

Sandwich types	Reference	Peak force (kN)	SEA (J/g)
GG core sandwich	Current study	3.1	0.76
GK core sandwich	Current study	3.3	0.93
GZ core sandwich	Current study	3.8	1.01
Expanded Polypropylene foam (EPP-F) core sandwich	[51]	2.3	0.8
Aluminium honeycomb (Al-H) core sandwich	[51]	2.4	0.8
Rubber ball (R-B) core sandwich	[51]	5.8	0.2
Plastic ball (P- B) core sandwich	[51]	2.8	0.6

30 J exhibited a very similar load-displacement response compare to the non-impacted specimens. However, the load carrying capacity of GG sandwich reduced by 63% and 79% and stiffness dropped by 75% and 89% at 40 J and 50 J, respectively due to the core fracture. The bending resistance of the GK sandwich core also decreased with the increase of impact energy due to the existence of core struts damage. The capacity of GK decreased by 37% and 60%, and stiffness dropped by 17% and 25% at 40 J and 50 J, respectively. On the other hand, the GZ sandwich showed better resistance when comparing with GG and GK. The bending loads capacity reduced by 15% and 23% and the stiffness was dropped by 2% and 20% at 40 J and 50 J, respectively for GZ sandwich. This is due to the replacement of one layer GG fibre by the high-performance GZ fibre that increased impact resistance and protected the core from the damaging effect of impact force.

Fig. 11 shows of the residual load-strain response on the upper face sheet of the corrugated core sandwiches under four-point bending after low-velocity impact. All specimens except GG at 40 J and 50 J showed tensile strain (Fig. 11a to c) in the upper face sheet of the sandwiches.

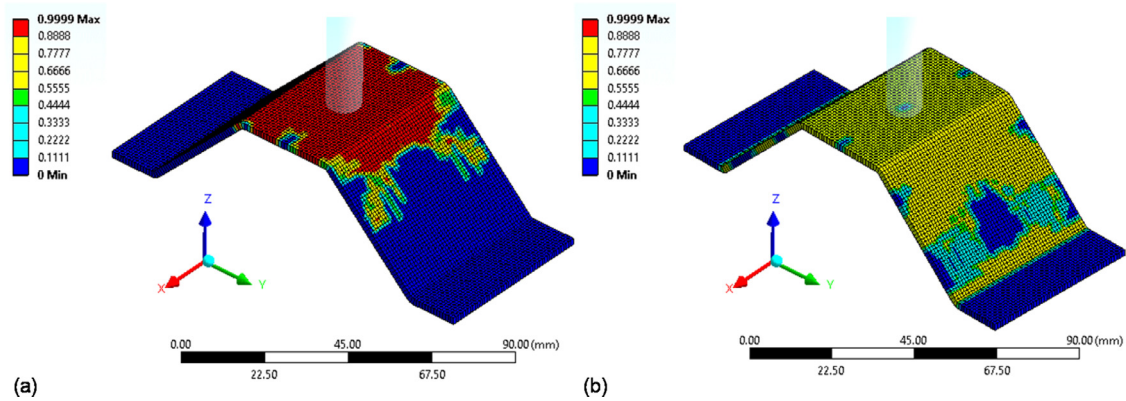


Fig. 9. Stress distribution based on failure criteria of the composite sandwich core, (a) GG sandwich core, and (b) ZG sandwich core.

This tensile strain at the middle of the upper skin can be attributed to the upward bending of the upper skin (Fig. 11d) due to the high resistance of the core even after impact that is confirming the superior performance of the fibre composite core. On the other hand, the compressive strain in GG sandwich at 40 J and 50 J (Fig. 11a) is due to the core rupture followed by de-bonding between upper skin and core when subjected to low-velocity impact that created positive moment (compressive strain) at the upper skin under four-point bending.

Fig. 12(a) shows the variation of the residual capacity of the GG, GK, and GZ sandwiches with respect to impact energy. At 30 J, the residual capacity of all specimens is very similar to the initial strength. This is due to the low level of applied energy, which is just above the threshold limit, as discussed before. A significant drop was noticed between 30 J and 40 J because the specimen exhibited de-bonding and buckling at 40 J. However, the reduction of the capacity was comparatively lower between 40–50 J than 30–40 J as no major changes in failure mode were observed between 40–50 J, as indicated in Table 4. Fig. 12(b) normalised the variation of the residual capacity with respect to the applied energy. This normalised variation is useful to compare the rate of changes in the capacity with applied energy. It can be seen that the rate of reduction of the capacity is the lowest for GZ followed by GK and GG. In other words, at 50 J kinetic energy, the residual strength and stiffness of GZ is 37% and 5% more than GK and 56% and 69% more than GG combination, respectively. This implies the replacement of one layer of glass fibre by the high-performance Zylon is effective in maintaining the initial capacity of the composite trapezoidal corrugated core sandwich structures.

4.6. Empirical modelling

Experimentation is the preferred choice to understand the residual capacity after the impact event of the hybridised corrugated core sandwich structures. However, a systematic reduction of a large number of data points and multiple curve fitting to reduced data to parameter model has been developed for prediction of the residual capacity of the structure. Fig. 12(b) showed the variation of normalised

residual capacity (F/F_0) with the increase of impact energy which can be predicted by Eq. (1). In Eq. (1), α and β are the material constants while E is the kinetic energy of the impactor. The material constant α is the function of β which can be determined by Eq. (2). The magnitude of β is dependent on the impact strength of the material and an increase of impact capacity reduce the β value. In the present study, the magnitude of β is 1 for GG that reduced to 0.54 for the GK and 0.15 for GZ sandwich. It is worth mentioning that Eqs. (1) and (2) were developed based on the kinetic energy ranged from 30 J to 50 J. Table 6 calculated the residual capacity using an empirical equation and compared it with the experimental results. It can be seen that the empirical equation can estimate the residual capacity within 10% of the experimental results. However, this slight variation of the result is due to the estimation of β , using a limited number of experimental impact strength results.

$$\frac{F}{F_0} = 7\alpha e^{-\beta E} \tag{1}$$

$$\alpha = 0.15e^{1.9\beta} \tag{2}$$

The proposed model can be improved further by considering the effect of a multi-layer replacement instead of one ply examined in the current study. Moreover, the influence of a wide range of impact energy, geometric parameters and material properties need to be included for establishing a robust model. Further studies are recommended in the aforementioned areas.

5. Conclusions

Low-velocity impact behaviour of corrugated sandwich panels fabricated with glass fibre core and hybridised using Kevlar and high-performance Zylon fibres (Glass-to-Kevlar and Glass-to-Zylon ratio is 75:25) were investigated. The impact behaviour, damage modes, and energy dissipation of the sandwiches were studied and the residual load carrying capacity after impact were investigated using four-point bending test from which the following conclusions are drawn:

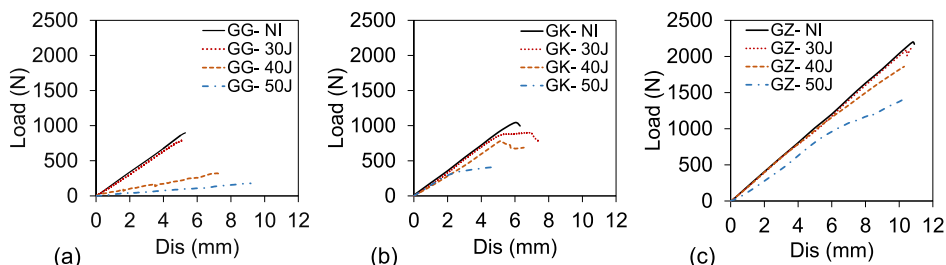


Fig. 10. Force-displacement response of non-impacted and impacted panels under four-point bending (a) GG, (b) GK, and (c) GZ.

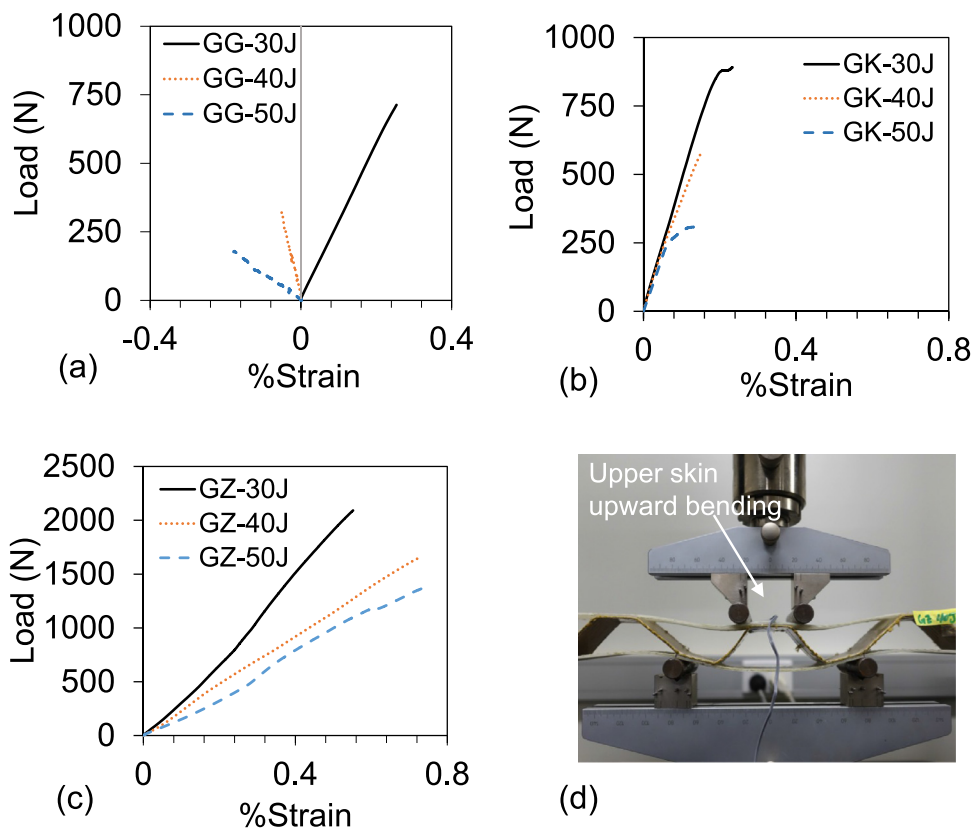


Fig. 11. Load-strain response of the corrugated core sandwich under four-point bending after impact a) GG, b) GK, c) GZ and (d) upward bending of the upper skin.

- The concept of hybridising glass fibre core with high-performance Zylon is more effective when sandwich panels are subjected to an impact energy well above the threshold limit for damage.
- Replacing one layer out of four layers (i.e., 25% replacement) of the glass fibre by Kevlar or Zylon fibres eliminated severe core failure. Moreover, the core failure in Glass-Glass combination is internal that is difficult to detect by visual inspection. This limitation can be overcome by Glass-Zylon hybridisation as the failure is external due to their superior energy absorption ability.
- Glass-Zylon hybridisation distributed the impact force in the wider area on the upper face sheet compare to Glass-Kevlar or Glass-Glass combination. This distribution minimised stress concentration and enhanced impact capacity of the corrugated core sandwich structures as shown by finite element modelling.
- Employing high-performance ply in the sandwich core provided high specific energy absorption without increasing structural weight. Glass-Kevlar and Glass-Zylon combination offered better specific energy absorption than the other traditional core materials

Table 6

Comparison between experimental and empirical results.

Sandwich type	Experimental, (F/F_o)	Empirical Eq. (F/F_o)	% Variation
GG-30J	0.839	0.807	3.9
GG-40J	0.368	0.392	6.4
GG-50J	0.205	0.191	7.2
GK-30J	0.876	0.872	0.5
GK-40J	0.630	0.591	6.2
GK-50J	0.403	0.400	0.9
GZ-30J	0.963	1.01	4.8
GZ-40J	0.845	0.908	7.3
GZ-50J	0.773	0.801	3.6

such as expanded polypropylene, aluminium, rubber and plastic.

- The loss of strength and stiffness of corrugated core sandwich structures due to an impact event is lower in Glass-Zylon hybridisation than Glass-Kevlar and Glass-Glass combination. At applied energy of 50 J, the residual strength and stiffness of Glass-

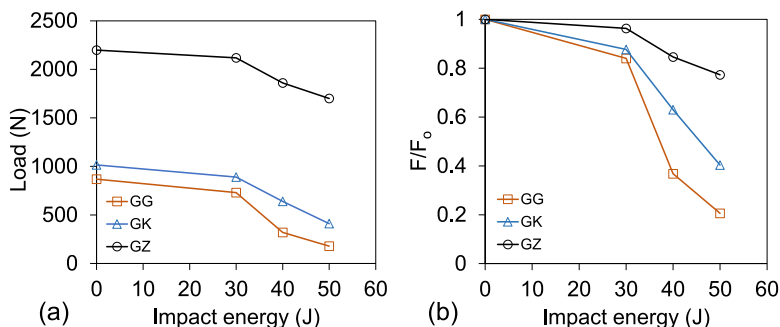


Fig. 12. Residual strength of the GG, GK, and GZ sandwich under four-point bending a) residual capacity vs. impact energy, and b) normalised residual capacity vs impact energy.

Zylon is 37% and 5% more than Glass-Kevlar and 56% and 69% more than Glass-Glass combination, respectively. The proposed empirical equations estimated the residual capacity within 10% accuracy.

Further development of finite element analysis would require in-depth investigation with different stacking sequences of the high-performance ply in order to understand the effect of ply orientations.

Declaration of Competing Interest

The authors declare that they have no conflict of interest regarding the publication of this manuscript.

Acknowledgments

The first author would like to thank the Ministry of Higher Education, Iraq, for their financial support. The authors also would like to appreciate the experimental support from the technical staff in the laboratory of Centre for Future Materials (CFM), University of Southern Queensland, Australia.

References

- Ferdous W, Manalo A, Aravinthan T, Fam A. Flexural and shear behaviour of layered sandwich beams. *Constr Build Mater* 2018;173:429–42.
- Aminanda Y, Castanié B, Barrau JJ, Thevenet P. Experimental and numerical study of compression after impact of sandwich structures with metallic skins. *Compos Sci Technol* 2009;69:50–9.
- Williams HR, Trask RS, Bond IP. Self-healing sandwich panels: restoration of compressive strength after impact. *Compos Sci Technol* 2008;68:3171–7.
- Xie WH, Meng SH, Ding L, Jin H, Du SY, Han GK, et al. High-temperature high-velocity impact on honeycomb sandwich panels. *Compos Part B* 2018;138:1–11.
- Zhang J, Qin Q, Xiang C, Wang TJ. Dynamic response of slender multilayer sandwich beams with metal foam cores subjected to low-velocity impact. *Compos Struct* 2016;153:614–23.
- Wadley HNG, O'Masta MR, Dharmasena KP, Compton BG, Gamble EA, Zok FW. Effect of core topology on projectile penetration in hybrid aluminum/alumina sandwich structures. *Int J Impact Eng* 2013;62:99–113.
- St-Pierre L, Deshpande V, Fleck N. The low velocity impact response of sandwich beams with a corrugated core or a Y-frame core. *Int J Mech Sci* 2015;91:71–80.
- Deshpande VS, Fleck NA, Ashby MF. Effective properties of the octet-truss lattice material. *J Mech Phys Solids* 2001;49:1747–69.
- Li S, Yang J-S, Wu L-Z, Yu G-C, Feng L-J. Vibration behavior of metallic sandwich panels with hourglass truss cores. *Marine Struct* 2019;63:84–98.
- Dharmasena KP, Wadley HNG, Liu T, Deshpande VS. The dynamic response of edge clamped plates loaded by spherically expanding sand shells. *Int J Impact Eng* 2013;62:182–95.
- Kılıçaslan C, Güden M, Odacı İ, Taşdemirci A. Experimental and numerical studies on the quasi-static and dynamic crushing responses of multi-layer trapezoidal aluminum corrugated sandwiches. *Thin-Walled Struct* 2014;78:70–8.
- Dharmasena K, Queheillalt D, Wadley H, Chen Y, Dudd P, Knight D, et al. Dynamic response of a multilayer prismatic structure to impulsive loads incident from water. *Int J Impact Eng* 2009;36:632–43.
- Zhang L, Hebert R, Wright JT, Shukla A, Kim J-H. Dynamic response of corrugated sandwich steel plates with graded cores. *Int J Impact Eng* 2014;65:185–94.
- Boonkong T, Shen YO, Guan ZW, Cantwell WJ. The low velocity impact response of curvilinear-core sandwich structures. *Int J Impact Eng* 2016;93:28–38.
- Eyvazian A, Najafian S, Mozafari H, Kumar AP. Crashworthiness analysis of a novel aluminum bi-tubular corrugated tube—experimental study. *Advances in manufacturing processes*. Springer; 2019. p. 599–607.
- Hou S, Zhao S, Ren L, Han X, Li Q. Crashworthiness optimization of corrugated sandwich panels. *Mater Des* 2013;51:1071–84.
- Zhang P, Liu J, Cheng Y, Hou H, Wang C, Li Y. Dynamic response of metallic trapezoidal corrugated-core sandwich panels subjected to air blast loading – An experimental study. *Mater Des* 2015;65:221–30. (1980–2015).
- Dayyani I, Shaw AD, Saavedra Flores EI, Friswell MI. The mechanics of composite corrugated structures: a review with applications in morphing aircraft. *Compos Struct* 2015;133:358–80.
- Zhang J, Supernak P, Mueller-Alander S, Wang CH. Improving the bending strength and energy absorption of corrugated sandwich composite structure. *Mater Des* 2013;52:767–73.
- Hu Y, Li W, An X, Fan H. Fabrication and mechanical behaviors of corrugated lattice truss composite sandwich panels. *Compos Sci Technol* 2016;125:114–22.
- Ferdous W, Ngo TD, Nguyen KTQ, Ghazlan A, Mendis P, Manalo A. Effect of fire-retardant ceramic powder on the properties of phenolic-based GFRP composites. *Compos Part B* 2018;155:414–24.
- Wadley HNG, Dharmasena KP, O'Masta MR, Wetzel JJ. Impact response of aluminum corrugated core sandwich panels. *Int J Impact Eng* 2013;62:114–28.
- Hou S, Li T, Jia Z, Wang L. Mechanical properties of sandwich composites with 3d-printed auxetic and non-auxetic lattice cores under low velocity impact. *Mater Des* 2018;160:1305–21.
- Li T, Wang L. Bending behavior of sandwich composite structures with tunable 3D-printed core materials. *Compos Struct* 2017;175:46–57.
- Odacı İ, Kılıçaslan C, Taşdemirci A, Güden M. Projectile impact testing of glass fiber-reinforced composite and layered corrugated aluminium and aluminium foam core sandwich panels: a comparative study. *Int J Crashworthiness* 2012;17:508–18.
- Mozafari H, Khatami S, Molatefi H. Out of plane crushing and local stiffness determination of proposed foam filled sandwich panel for Korean tilting train ePress – numerical study. *Mater Des* 2015;66:400–11.
- Susainathan J, Eyma F, De Luycker E, Cantarel A, Castanie B. Experimental investigation of impact behavior of wood-based sandwich structures. *Compos Part A* 2018;109:10–9.
- Ullah I, Elambasseril J, Brandt M, Feih S. Performance of bio-inspired Kagome truss core structures under compression and shear loading. *Compos Struct* 2014;118:294–302.
- He W, Liu J, Tao B, Xie D, Liu J, Zhang M. Experimental and numerical research on the low velocity impact behavior of hybrid corrugated core sandwich structures. *Compos Struct* 2016;158:30–43.
- Shin KB, Lee JY, Cho SH. An experimental study of low-velocity impact responses of sandwich panels for Korean low floor bus. *Compos Struct* 2008;84:228–40.
- He W, Liu J, Wang S, Xie D. Low-velocity impact response and post-impact flexural behaviour of composite sandwich structures with corrugated cores. *Compos Struct* 2018;189:37–53.
- Stapleton SE, Adams DO. Structural enhancements for increased energy absorption in composite sandwich structures. *J Sandw Struct Mater* 2011;13:137–58.
- Xiong J, Vaziri A, Ma L, Papadopoulos J, Wu L. Compression and impact testing of two-layer composite pyramidal-core sandwich panels. *Compos Struct* 2012;94:793–801.
- Schneider C, Kazemahvazi S, Zenkert D, Deshpande VS. Dynamic compression response of self-reinforced poly(ethylene terephthalate) composites and corrugated sandwich cores. *Compos Part A* 2015;77:96–105.
- Shi S, Sun Z, Hu X, Chen H. Flexural strength and energy absorption of carbon-fiber-aluminum-honeycomb composite sandwich reinforced by aluminum grid. *Thin-Walled Struct* 2014;84:416–22.
- Toyobo. ZYLON®(PBO fiber) technical information. 2005. in, Japan.
- Huang YK, Frings PH, Hennes E. Mechanical properties of zylon/epoxy composite. *Compos Part B* 2002;33:109–15.
- Cunniff PM, Auerbach MA. High performance “M5” fiber for ballistics/structural composites. *Proceedings of the 23rd army science conference*. 2002.
- Techniglu. Adhesives/R5 toughened. ATL composites Pty Ltd; 2017.
- Colan-Australia. Composite reinforcements fabric and tape product range, www.colan.com.au, in, 2017.
- Toyobo, PBO fiber zylon - technical information about zylon, www.toyobo.co.jp/in, Japan, 2005, pp. 1–18.
- Gurit, Guide to composites, www.gurit.com, in, Switzerland, 2018, pp. 1–74.
- Michigan-Tech, Mechanical properties data, in, www.mse.mtu.edu, USA, 2019.
- Fernández-Toribio JC, Alemán B, Ridruejo Á, Vilatela JJ. Tensile properties of carbon nanotube fibres described by the fibrillar crystallite model. *Carbon* 2018;133:44–52.
- Liu J, He W, Xie D, Tao B. The effect of impactor shape on the low-velocity impact behavior of hybrid corrugated core sandwich structures. *Compos Part B* 2017;111:315–31.
- ASTM-D7136. Standard test method for measuring the damage resistance of a fiber-reinforced polymer matrix composite to drop-weight impact event. *ASTM International*. 2012.
- Davies G, Olsson R. Impact on composite structures. *Aeronaut J* 2004;108:541–63.
- Jang BP, Huang CT, Hsieh CY, Kowbel W, Jang BZ. Repeated impact failure of continuous fiber reinforced thermoplastic and thermoset composites. *J Compos Mater* 1991;25:1171–203.
- ASTM-D5467/D5467M. Standard test method for compressive properties of uni-directional polymer matrix composite materials using a sandwich beam. *ASTM International USA*. 2017.
- ASTM-C393. Standard test method for Core shear properties of sandwich constructions by beam flexure. *ASTM international*. 2011. p. 8.
- Zhang Y, Zong Z, Liu Q, Ma J, Wu Y, Li Q. Static and dynamic crushing responses of CFRP sandwich panels filled with different reinforced materials. *Mater Des* 2017;117:396–408.